ELSEVIER

Chemical Engineering Journal 78 (2000) 131–139

Chemical Engineering Journal

www.elsevier.com/locate/cej

Physical modelling and numerical simulation of velocity fields in rotating disc contactor via CFD simulation and LDV measurement☆

W.Y. Fei, Y.D. Wang*, Y.K. Wan

Solvent Extraction Laboratory, The State Key Laboratory of Chemical Engineering, Department of Chemical Engineering, Tsinghua University, Beijing 100084, PR China

Received 25 January 1999; received in revised form 1 October 1999; accepted 5 October 1999

Abstract

Velocity fields in a rotating disc contactor (RDC) with single-phase flow have been measured using a Laser Doppler Velocimeter (LDV) and simulated with computational fluid dynamics software. Simulated velocity profiles are in fair agreement with the experimental ones. Both experimental and calculated results show that there exist vortices between adjacent rotating discs and between adjacent stator rings in the flow system. The vortex between stator rings enhances mixing and mass transfer in a compartment, while the vortex between discs is the main factor causing axial mixing. In order to suppress the axial mixing thus enhancing the mass transfer efficiency in the extraction column, a modified rotating disc contactor (MRDC) is proposed. Simulated velocity profiles in the new extraction column have shown that the axial mixing between the discs has been effectively eliminated.

Keywords: Extraction; Rotating disc contactor; Computational fluid dynamics; Mass transfer

1. Introduction

Liquid–liquid extraction is an important separation technology in the process industries. The Rotating disc contactor (RDC) is one of the major extraction columns which has been widely used in petroleum refining, chemical and metallurgical industries for its high throughput, low investment, easy operation and maintenance. But due to limitations of its design, mass transfer efficiency of commercial RDC is low, especially for very low interfacial tension systems, and the axial back-mixing is severe. Axial mixing is the undesirable forward- and back-mixing of the continuous and dispersed phases as they pass through the extraction column. The ideal situation is pure plug flow of the two phases as they pass each other in the column, which maximises the concentration driving force. The effect of axial mixing is seen as concentration 'jumps' at either end of extractor. These jumps move the equilibrium and operating lines closer together, thus reducing concentration driving force and increasing the stage requirement in the extractor [1]. Some reports [2] showed that 60–75% of RDC height is used to compensate the decrease of mass transfer efficiency, and another report describes a commercial size RDC which has just three theoretical stages [3]. Therefore, it becomes an imperative research task to improve the mass transfer efficiency of RDC, to strive for high capacity while minimising axial mixing. A lot of work [4,5] had been done on RDCs, by chemical engineering researchers. This work can be divided into two classes, one is concerned with the mass transfer performance and hydrodynamics such as throughout capacity, drop diameter distributions, flooding velocities with varied systems and RDC scaling. The main objective of this category is to seek for the optimal operating conditions and design method. Many correlations have been presented in the literature, but when the system or column scale changes, the use of these correlations is quite limited. Another class of papers is concerned with optimising the design of the RDC. Several modified RDCs, such as asymmetric rotating disc extractor (ARD) [6], the enhanced coalescence column (EC) [7], self-stabilising high performance extractor (SHE) [8], open turbine rotating disc contactor (OTRDC) [9] have been presented. However, major changes in the RDC's inner design were needed in order to achieve better mass transfer performance, usually at the expense of throughout capacity decrease.

Computational fluid dynamics (CFD) has been applied in automobile and aerospace industries successfully for decades. Its use in chemical engineering has yielded interesting results for concentrates mostly on stirred tanks

☆Project supported by the National Natural Science Foundation of China (29836130).

*Corresponding author.

1385-8947/00/$ – see front matter
PII: S1385-8947(00)00156-X

Table 1
RDC structure parameters for LDV measurements

Parameter	Symbols	Value (m)	Parameter	Symbols	Value (m)
RDC inner diameter	D_T	0.29	Stator ring inner diameter	D_R	0.19
Rotating disc diameter	D_r	0.174	Compartment height	H_C	0.078
Shaft diameter	D_S	0.014	Column height	H_T	0.46

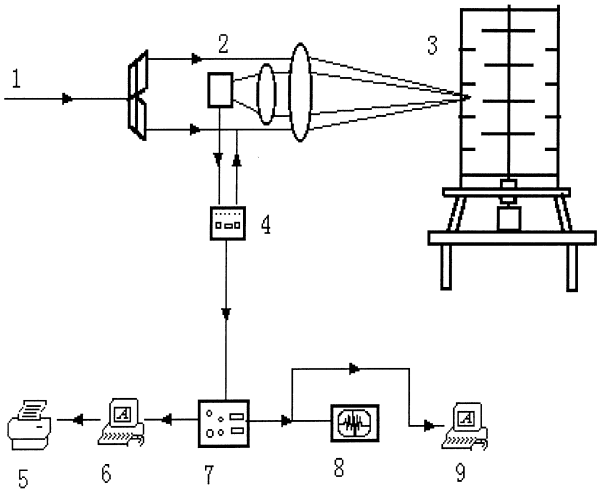

1. He-Ne Laser. 2. Photomultiplier. 3. RDC column. 4. Frequency shifter. 5. Printer. 6. HP computer. 7. Signal processor. 8. Oscilloscope. 9 IBM computer.

Fig. 1. Schematic diagram of LDV measuring system.

[10]. Velocity field measurements by LDV and numerical simulations using CFD have been performed by Weiss and Bart [11], Bart et al. [12], Rieger et al. [13,14] in a small column with a diameter of 150 mm. Xu and Fei [15] measured velocity profiles in a rotating disc contactor with a diameter of 100 mm. Up till now, most of the velocity field measurement has been done with small column diameters. Since two-phase flow in a RDC is very complicated, the majority of the experimental measurements of the velocity fields were in a single phase, and mostly the measurement system is water. Although two-phase flow fields have been done [14], there are still some uncertainties in the two-phase

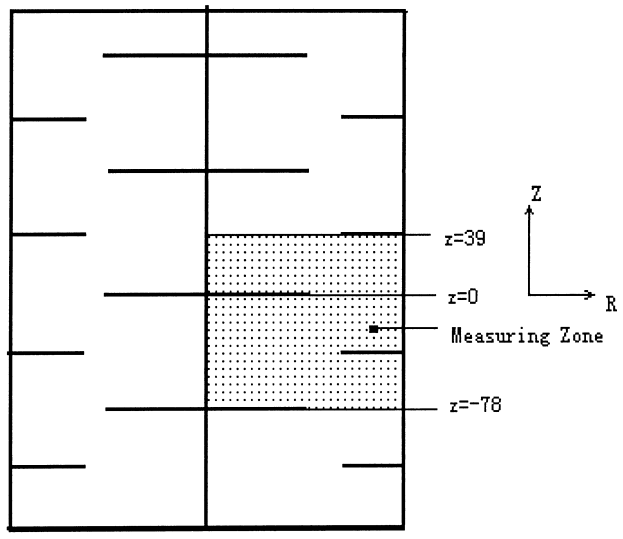

Fig. 2. Measuring zone inside the RDC.

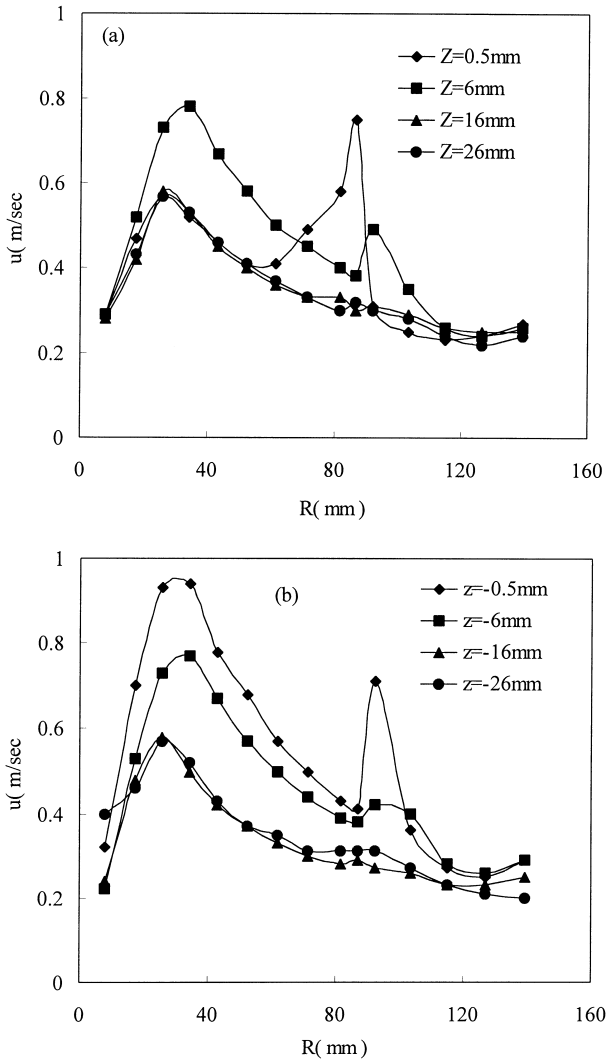

Fig. 3. Measured tangential velocity profiles without circulation flow: N=300 rpm. (a) Upper half of the compartment; (b) lower half of the compartment.

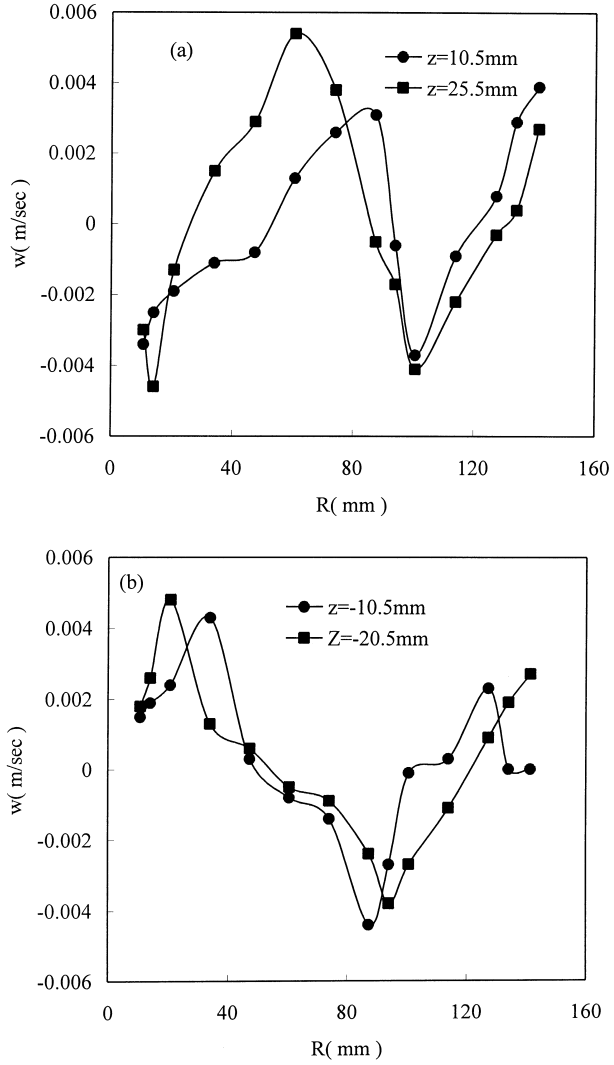

Fig. 4. Measured axial velocity profiles without circulation flow: N=300 rpm. (a) Upper half of the compartment; (b) lower half of the compartment.

flow measurements. There is no report on velocity field measurements in pilot-scale and on modifying the inner structure of the RDC so as to change the flow pattern and increase the mass transfer performance.

In this study, tangential and axial velocity fields in a pilot-scale RDC have been measured and simulated using CFD software. Our specific objective is to get a deeper understanding of the flow pattern inside a RDC. We try to locate the areas where axial mixing happens and how to eliminate them by modifying the inner structure of the RDC.

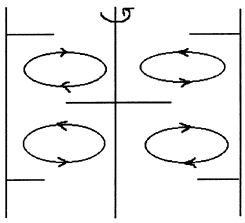

Fig. 5. Schematic diagram of the flow pattern: N=300 rpm; Q=0 m^3/s.

2. Experimental

A pilot-scale RDC was designed and constructed with four compartments, its parameters are showed in Table 1. The column was made of glass pipe and inner parts were made of aluminium, the rotating discs and shaft was driven by a 0.2 kW motor and its speed was controlled by a speed regulator from 0 to 1500±2 rpm. A photoelectric speed detector measured the rotation speed. The measuring system used was TSI9100-3 Laser Doppler Velocimeter (LDV). The single channel LDV system signal processor was 1980B, later

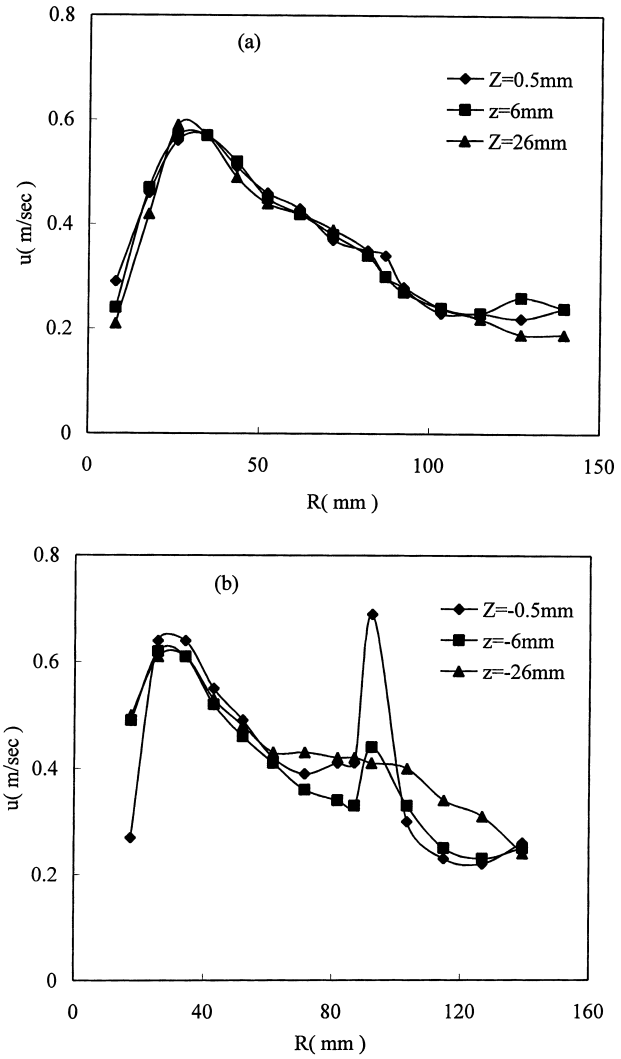

Fig. 6. Measured tangential velocity profiles: N=300 rpm, Q=4.44×10^{-4} m^3/s. (a) Upper half of the compartment; (b) lower half of the compartment.

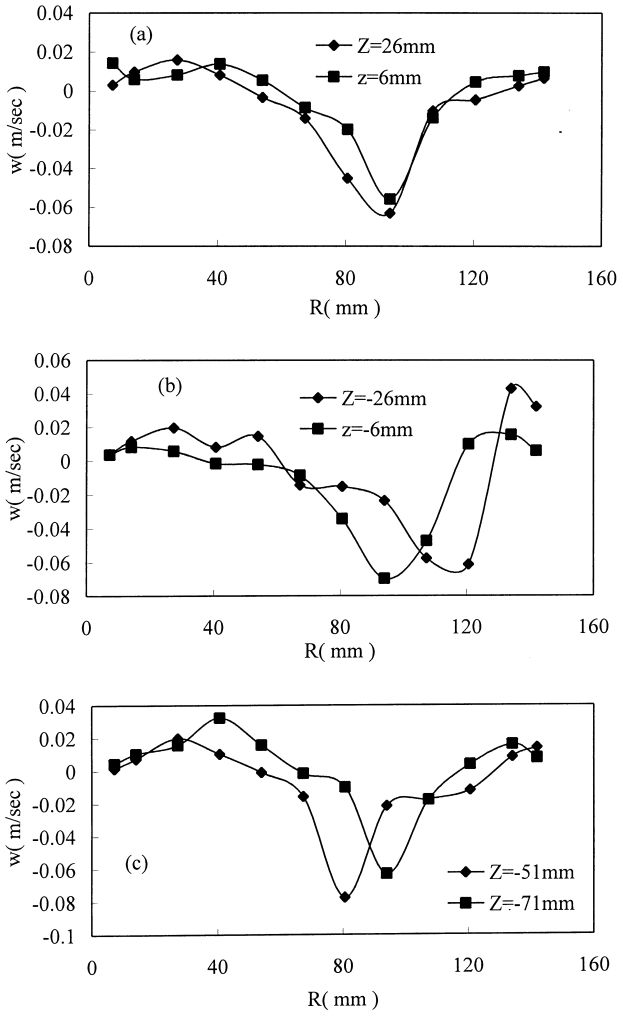

Fig. 7. Measured axial velocity profiles: N=300 rpm, Q=4.44×10^{-4} m^3/s. (a) Upper half of the compartment; (b) lower half of the compartment; (c) upper half of the adjacent compartment.

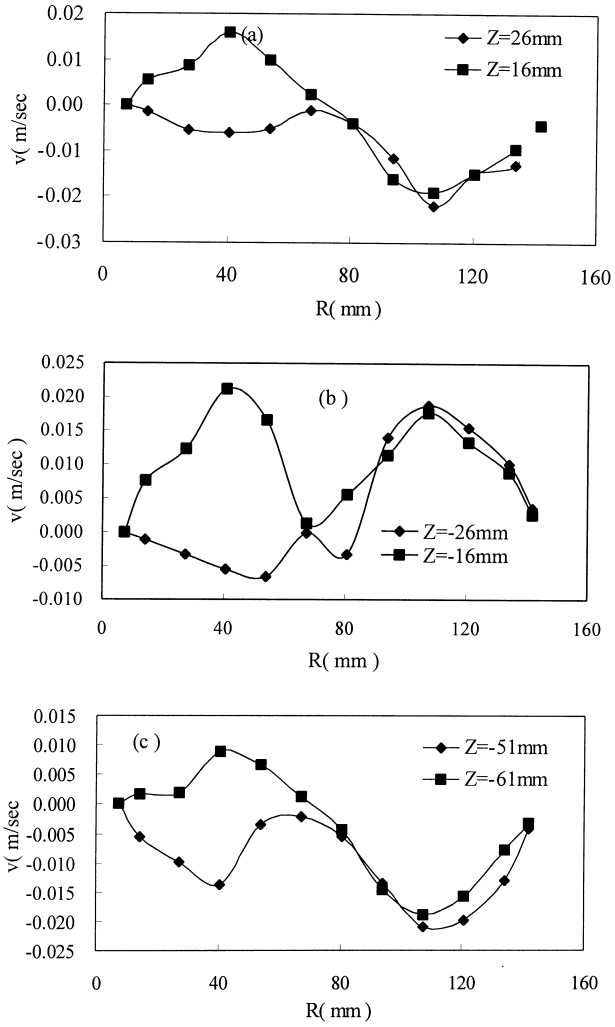

Fig. 8. Measured radial velocity profiles: N=300 rpm, Q=4.44×10^{-4} m^3/s. (a) Upper half of the compartment; (b) lower half of the compartment; (c) upper half of the adjacent compartment.

replaced with QSP LDA processor. A schematic diagram of the measuring system is shown in Fig. 1. A circulation flow system was installed with the flow in at the top of the column and out at the bottom of the column. The flow rate is controlled by a valve and measured by a rotameter from 0 to 1.6 M^3/h. The pipeline of the flow system was cooled in order to maintain constant temperature of the fluid. The system is so designed to investigate the single phase flow of pure water with and without throughflow. Fine polystyrene particles are added as seeding particles to increase the signal intensity. To reduce reflecting light, all the inner parts of the RDC are blackened, and a backscatter collection method is adopted for the limit of structure.

The measuring zone (shaded area) is depicted in Fig. 2. Only one compartment and nine different horizontal levels (Z=39, 26, 16, 6, 0.5, 0, −0.5, −6, −16, −26, −39 mm, where Z=0 refer to disc level in a compartment) were chosen to measure tangential velocity. Frequency shift technology is used to measure axial velocity and determine the axial velocity direction, the frequency shifter is TSI 9186A. In order to investigate the flow behaviour in and between compartments, 14 horizontal levels (Z=26, 16, 6, 0.5, 0, −0.5, −6, −16, −26, −39, −51, −61, −71, −78 mm) in one and a half compartments were chosen to measure axial velocity.

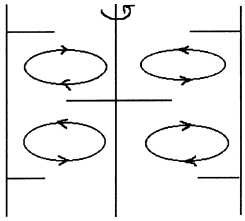

Fig. 9. Schematic diagram of the flow pattern: N=300 rpm, Q=4.44×10^{-4} m^3/s.

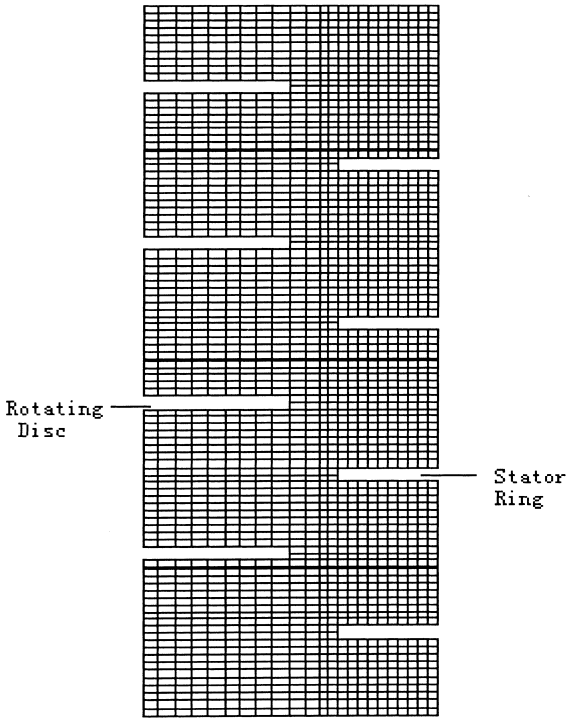

Fig. 10. Section of the simulation grids in an RDC.

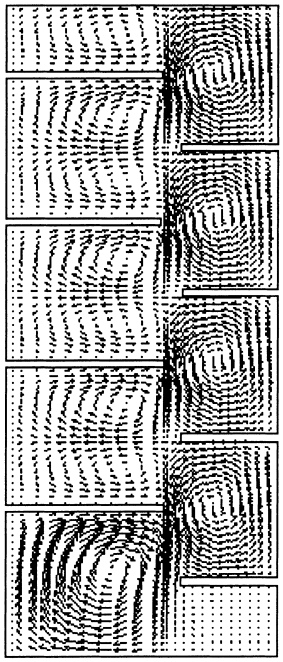

Fig. 12. Simulated velocity profiles: N=300 rpm, Q=0 m^3/s.

Doppler signals received were processed using model 1980B Counter-type signal processor as well as QSP LDA processor.

2.1. Mathematical model

Steady-state, axial-symmetric Navier–Stokes equations written for an incompressible Newtonian fluid in steady-state flow were used.

The boundary conditions for the given problems are:
At the surface of the rotating disc and central shaft

$$u = \frac{2\pi rN}{60} \tag{1}$$

$$v = w = 0 \tag{2}$$

At the rest of the solid boundaries

$$u = v = w = 0 \tag{3}$$

At the inlet of the column

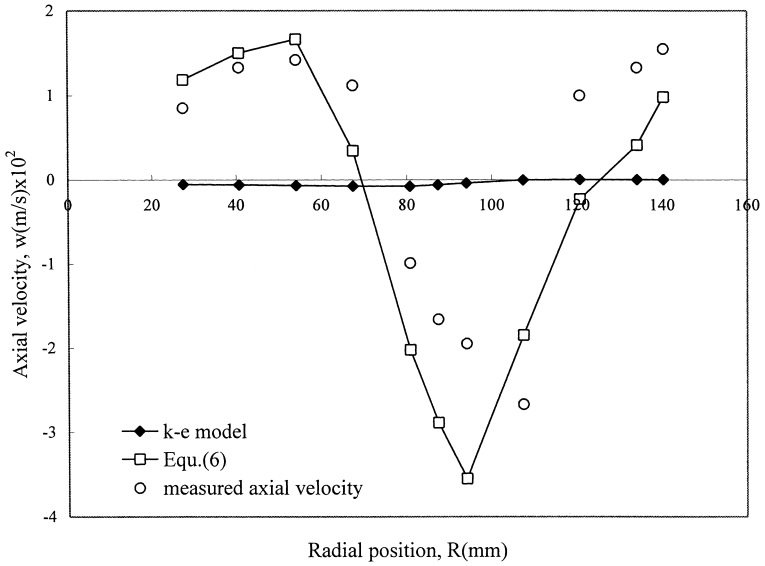

Fig. 11. Comparative simulation results of the two turbulence models (N=300 rpm, Q=4.44×10^{-4} m^3/s, Z=−6 mm).

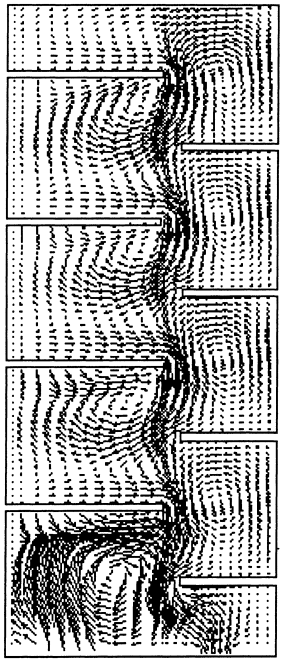

Fig. 13. Simulated velocity profiles: N=300 rpm, Q=2.22×10^{-4} m^3/s.

$$w = \frac{Q}{4\pi D_T^2} \tag{4}$$

At the outlet of the column

$$w = \frac{Q}{4\pi D_e^2} \tag{5}$$

where u is the tangential velocity (m/s), v the radial velocity (m/s), w the axial velocity (m/s), r denotes the radial distance (m), N represents the rotation speed (rpm), D_e the diameter of liquid outlet (m), D_T the diameter of the RDC (m), Q represents the liquid flow rate (m^3/s).

In this study, the minimum rotation speed of the disc is 100 rpm. At such a condition, the Reynolds number is $\mathrm{Re} = (\rho D_R^2 N)/\mu = 49470.6$, where D_R is the disc diameter. Therefore, the fluid flow inside the RDC is in a turbulent flow regime. The following equation was adopted to calculate the turbulent viscosity [16]

$$\mu_t = 0.01 D_T^2 \omega \tag{6}$$

where ω is angular speed of the disc. Other turbulence models like the k-ε model were also tested and the result will be presented in Section 3.

The calculations were done with the commercial CFD package PHOENICS.

3. Results and discussion

The three velocity components, namely, tangential, radial and axial velocity profiles inside an RDC were measured with or without throughflow.

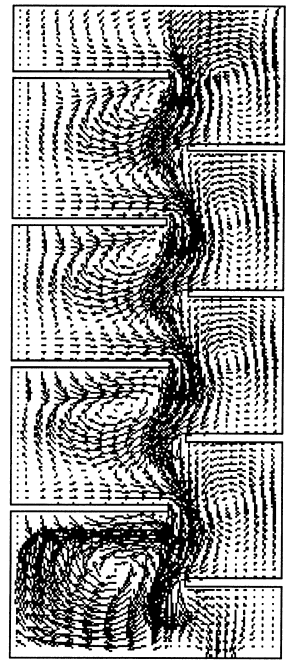

(a)

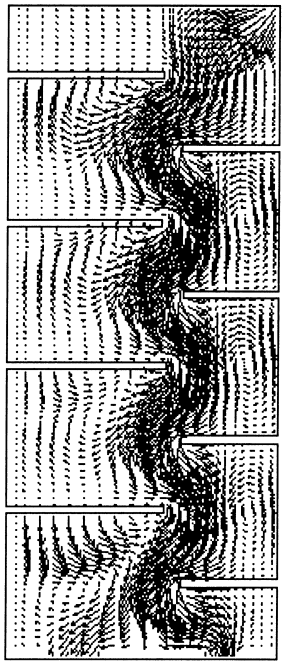

(b)

Fig. 14. Simulated velocity profiles. (a) N=300 rpm, Q=4.44×10^{-4} m^3/s. (b) N=100 rpm, Q=4.44×10^{-4} m^3/s.

Fig. 3 shows the measured tangential velocity profiles in one compartment at rotation speed of 300 rpm in the non-flow system. It is found that tangential velocity profiles close to disc (Z=6 to −6 mm) exhibit bimodal distributions which appear in the disc rim (R=87–94 mm) and near

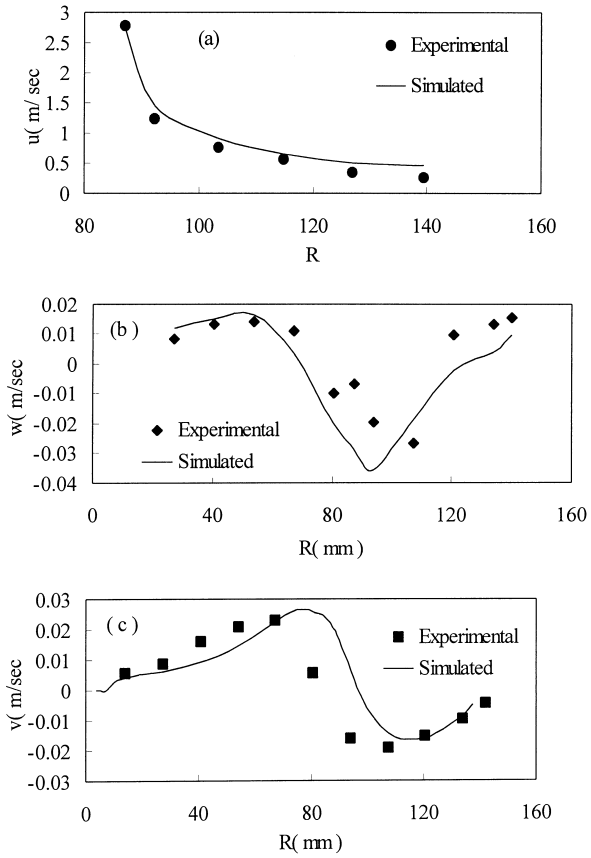

Fig. 15. Comparison between experimental and simulated velocity profiles. (a) Tangential (N=300 rpm, Q=0 m^3/s, Z=0 mm); (b) axial (N=300 rpm, Q=4.44×10^{-4} m^3/s, Z=−6 mm); (c) radial (N=300 rpm, Q=4.44×10^{-4} m^3/s, Z=17 mm).

rotating shaft (R=25–35 mm), out of this area, the tangential velocity profiles are just unimodal distributions. Fig. 4 illustrates measured axial velocity profiles at rotation speed of 300 rpm without circulation flow, in which the axial flow is positive upward and negative downward. It can be seen that in the upper half of the compartment, flow can be divided into four regions. At R=7–25 mm and R=95–120 mm, flows are downward, and at R=25–95 mm and $R\geq$120 column wall, flows are upward. The upward flow near the column wall is constrained by stator rings turns towards the centre of the column. It meets the upward flow induced from centrifugal force of rotating disc near the disc rim, then changes its direction downwards, the flow downward near the central shaft constrained by rotating disc will move towards the disc rim. As a result, a vortex forms in the region of central shaft to disc rim. The flow pattern in a non-flow system is sketched in Fig. 5. The fluid in the boundary layer at the rotating disc is moving in tangential direction due to the action of viscous forces. Thereby the fluid is centrifuged radial outward at the disc inducing the so-called secondary flow. From flows in turbomachinary and from the analogy to flows in closed stirred vessels the radial secondary flow is expected to be further thrown outwards and after impinging on the outer column wall, to be reflected, moving then again inwards along the stator in direction back to the shaft.

For a flow system, measured velocity profiles are shown in Figs. 6–8. Velocity profiles exhibit a dramatic change between flow system and non-flow system. Tangential velocity profiles under the circulation flow condition (Fig. 6) is similar to that of non-flow case. However, axial velocity in the open area between the rotating disc rims and stator rings is much higher than that of non-flow system. The upward flows near the column wall and central shaft form two vortices with the main downward axial flow (Fig. 7). Fig. 8 shows that the radial flow is relatively smaller compared to the other two velocity components. The combination of the three velocity components is sketched in Fig. 9. There exist two vortices: one between stator rings and another between rotating discs. The vortex between the stator rings is caused by the rotation of the disc and the main flow. This vortex can

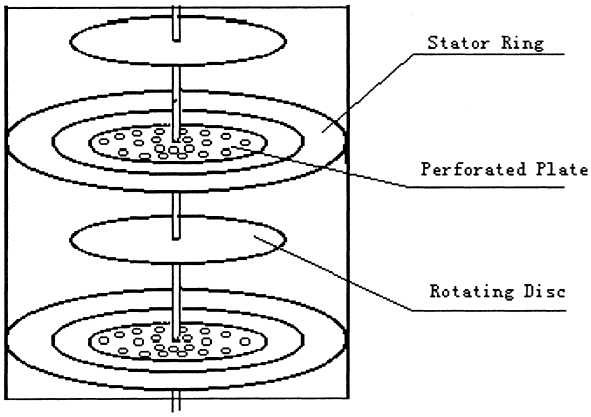

Fig. 16. Schematic diagram of MRDC.

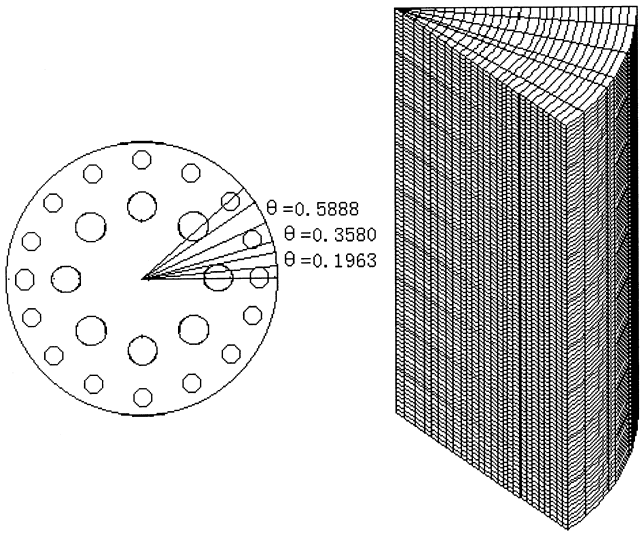

Fig. 17. Section of simulation grids for MRDC.

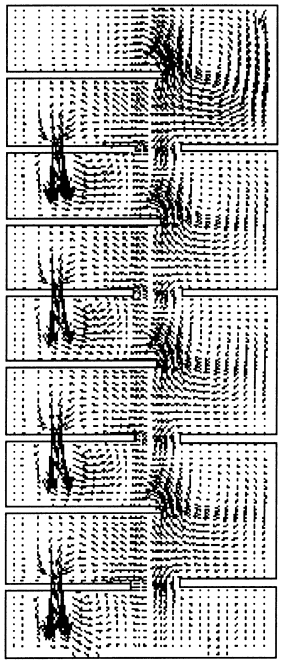

(a)

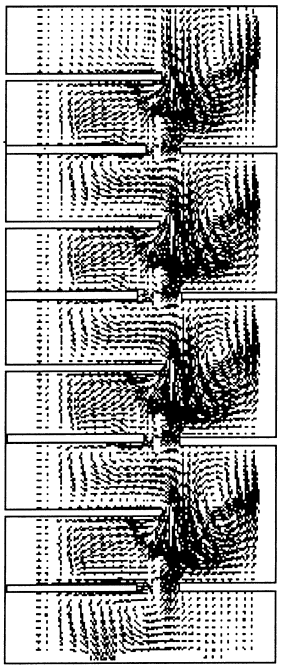

(b)

Fig. 18. Modified RDC flow pattern. (a) N=300 rpm, Q=4.44×10^{-4} m^3/s, θ=0.1963; (b) N=300 rpm, Q=4.44×10^{-4} m^3/s, θ=0.5888.

promote the mixing inside a compartment so as to enhance the mass transfer. The vortex between the rotating discs expands to the next compartment and is formed when the main flow meets the discs. It is probably one of the main reasons causing back-mixing inside a RDC column. The other cause of poor mass transfer in a flow system is the channelling flow.

Numerical simulations were then performed. The section of simulation grids is illustrated in Fig. 10. Two turbulence models were used one described by Eq. (6), and the other is the k–ε model. Simulation of axial velocity with two turbulence models is depicted in Fig. 11. It is shown that the simple turbulence model of Eq. (6) fits the experimental measurements better than the k–ε model. Fig. 12 shows the velocity profiles for non-flow system. It can be seen that there are three vortices within a compartment: one is between the stator ring; the other two above and below the rotating disc. These vortices promote the mixing in a compartment and are of benefit to the mass transfer. However, in a flow system, the vortex between the rotating disc is only becoming apparent as the flow rate increases (Figs. 13 and 14a). At low rotation speed (Fig. 14b), channelling flow takes the main role. The simulation results have the same outcome as the experimental ones. Selected experimental results are compared with the simulation in Fig. 15. The two results are in a good agreement.

The vortices between rotating discs are the main factors which caused axial back-mixing which should be eliminated for the benefit of higher mass transfer efficiency. A modified rotating disc contactor (MRDC) is, therefore, proposed as shown in Fig. 16. MRDC is different to the traditional RDC in that a perforated rotating disc is added at the stator ring level. The disc is perforated so that the throughput capacity of MRDC can be kept nearly as high as the RDC. Numerical simulations have been performed with MRDC. Simulation grids for MRDC are illustrated in Fig. 17. Simulated flow pattern of MRDC in Fig. 18 indicates that the vortex between the rotating discs has been effectively eliminated. Hydrodynamic and mass transfer experiments were carried out in both MRDC and RDC. The extraction column was 0.1 m diameter and contained 35 rotating discs. The effective column height was 1.0 m, rotating disc diameter 0.06 m, stator ring diameter 0.07 m, central shaft diameter 0.015 m, stainless steel disc and stator plate thickness 0.0012 m. In the case of MRDC experiments, perforated discs were installed between every two rotating discs. The continuous phase was deionised water having a density of 1000 kg/m^3 and viscosity of 1.610 mPa s. Dispersed phase was 6% (by weight) succinic acid in n-octanol having a density of 876.2 kg/m^3 and viscosity of 3.925 mPa s. The results shown in Fig. 19 indicates that mass transfer efficiency increased by 25–40% compared to conventional RDC while throughput capacity is only 1–3% lower than that of conventional RDC (Fig. 20).

4. Conclusion

Single phase velocity profiles in a pilot-scale rotating disc contactor have been measured using LDV and simulated by CFD software for both flow and non-flow systems. The simulated results agree fairly well with the experimental ones. There is a significant difference in flow pattern between

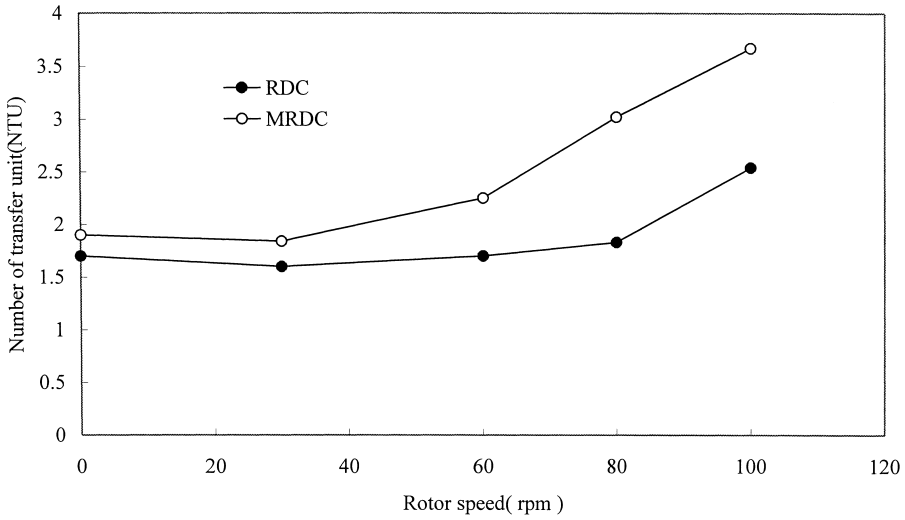

Fig. 19. Mass transfer comparison between MRDC and RDC (dispersed and continuous phase flow rate: $V_d=V_c=1.67\times10^{-5}\,m^3/s$).

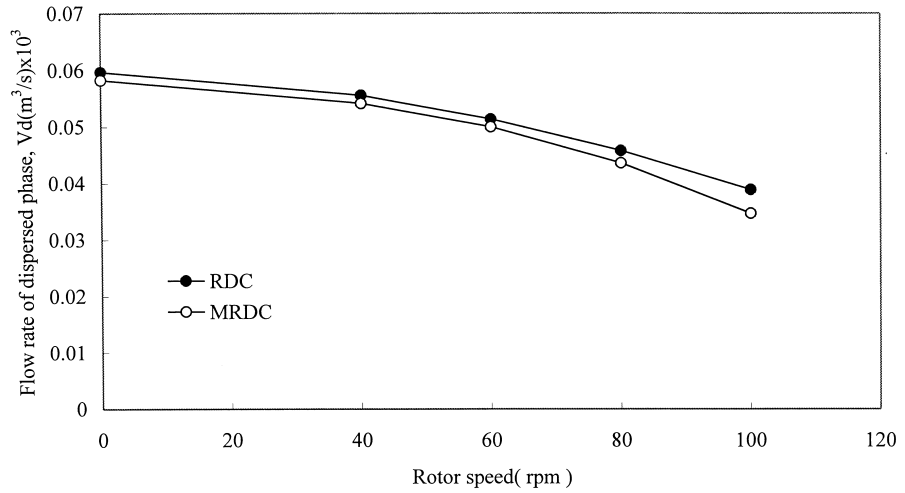

Fig. 20. Throughput capacity comparison between MRDC and RDC (flow rate of continuous phase, $V_c=1.67\times10^{-5}\,m^3/s$).

the two systems. The vortices occurred between the compartments are the main causes of axial mixing which has a significant effect on mass transfer efficiency in an RDC. To eliminate these vortexes and improve the mass transfer efficiency, a modified RDC (MRDC) is proposed. The experimental and simulated results have shown that vortices between the compartments can be effectively removed and mass transfer efficiency increased by 25–40% with MRDC.

References

[1] R.W. Cusack, P. Fremeaux, Chem. Eng. (New York) (1991) 132.
[2] T. Misek, V. Rod, Recent Advance in Solvent Extraction, Pergamon, New York, 1971, p. 197.
[3] S.Y. Ju, R.W. Pike, Can. J. Chem. Eng. 68 (1990) 3.
[4] W.J. Korchinsky, Rotating disc contactor, in: J.C. Godfrey, M.J. Slater (Eds.), Liquid–Liquid Extraction Equipment, Wiley, New York, 1994, p. 247.
[5] Z. Li, W. Fei et al., Liquid–Liquid Extraction Process and Equipment, Atomic Energy Press, Beijing, 1993, p. 478.
[6] T. Misek et al., Br. Chem. Eng. 15(2) (1970) 202.
[7] L. Steiner, S. Hartland, Chem. Rundsch 13 (1980) 256.
[8] W. Gaubinger, Ger. Chem. Eng. 6 (1983) 74.
[9] J.W. Zhu, Chem. Eng. Technol. 14 (1991) 167.
[10] A. Brucato et al., Chem. Eng. Sci. 53(21) (1998) 3653.
[11] C. Weiss, H.-J. Bart, in: Proceedings of ISEC'93, Vol. 2, Elsevier Applied Science, New York, 1993, p. 1191.
[12] H.-J. Bart, G. Husung, R. Marr, C. Weiss, in: Proceedings of the 11th International Congress Chem. Eng. Chem. Equip. Des. Auto., CHISA'93, 29 August–3 September 1993, Praha, Czech Republic, pp. A1–A11.
[13] R. Rieger, Comput. Chem. Eng. 18 (1994) s229.
[14] R. Rieger, H.-J. Bart, R. Marr et al., Comput. Chem. Eng. 20(12) (1996) 1467.
[15] H.Q. Xu, W.Y. Fei, J. Exp. Mech. (in Chinese) 10 (4) (1995) 316.
[16] H.I. Rosten, D.B. Spalding, Shareware PHOENICS Beginner's Guide — CHAM Report number TR100.